DEPENDENCE OF SECOND BREAKDOWN IN TRANSISTOR ON LOAD INDUCTANCE AND REVERSE BASE DRIVE

BY

MD. KAMRUL HASAN

A THESIS

SUBMITTED TO THE DEPARTMENT OF ELECTRICAL AND ELECTRONIC ENGINEERING, BUET, IN PARTIAL FULFILMENT OF THE REQUIREMENTS

FOR THE

DEGREE

MASTER OF SCIENCE IN ENGINEERING

DEPARTMENT OF ELECTRICAL AND ELECTRONIC ENGINEERING

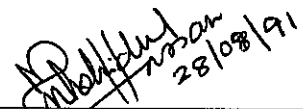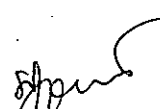BANGLADESH UNIVERSITY OF ENGINEERING AND TECHNOLOGY
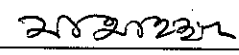
AUGUST, 1991.

THESIS TITLE   :" Dependence of Second Breakdown in Transistor
                          on Load Inductance and Reverse Base Drive "

Name of the Student : Md. Kamrul Hasan
Roll No   : 891349P, Session : 1987-88
Regd. No   : 83109

Accepted as satisfactory in the partial fulfilment of the
requirements for the degree of Master of Science in Engineering
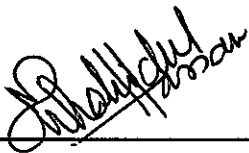(Electrical and Electronic).

BOARD OF EXAMINERS

1. _____   Chairman
   (Dr. M. M. Shahidul Hassan)   (Supervisor)
   Associate Professor
   Department of Electrical and
   Electronic Engineering, BUET,
   Dhaka-1000, Bangladesh.

2. _____   Member
   (Dr. Md. Mujibur Rahman)   (Ex-officio)
   Professor & Head
   Department of Electrical and
   Electronic Engineering, BUET,
   Dhaka-1000, Bangladesh.

3. _____   Member
   (Dr. Md. Rezwan Khan)
   Associate Professor
   Department of Electrical and
   Electronic Engineering, BUET,
   Dhaka-1000, Bangladesh.

4. _____   Member
   (Dr. Mohammad Ali Choudhury)
   Assistant Professor
   Department of Electrical and
   Electronic Engineering, BUET,
   Dhaka-1000, Bangladesh.

5. _____   Member
   (Dr. Md. Shamsuddin Ahmed)   (External)
   Professor & Head
   Department of Electrical and
   Electronic Engineering, ICTVTR,
   Board Bazar, Gazipur, Dhaka.

CERTIFICATE

This is to certify that this work has been done by me and it has not been submitted elsewhere for the award of any degree or diploma.

Countersigned   Signature of the student

(Dr. M. M. Shahidul Hassan)   (Md. Kamrul Hasan)
Supervisor

CONTENTS

ACKNOWLEDGMENTS

ABSTRACT

A major problem in epitaxial bipolar transistors in reverse biased conditions is the occurrence of current mode second breakdown(CSB). The base-current reversal may be brought by the conditions: i) operation above open-base breakdown voltage BV_{CEO} and ii) turn-off, during which excess charge is being extracted from the collector region. The lateral base current produces a voltage drop across the emitter-base junction. This has the effect of constricting the current to the center of the emitter diffusion. The constriction causes a rapid increase in the collector current density leading to CSB.

If the concentration of the space charge entering the collector exceeds the fixed thermally ionized impurity concentration, the mobile charge determines the electric field in the region. An applied voltage in presence of space charge limited current can develop a situation where the electric field will exceed its critical value for impact ionization resulting multiplication and localized breakdown. In this thesis, however, it is considered sufficient to calculate the pinch-in current density in the emitter and study the effects of the space charge in the collector region taking into consideration the critical voltage concurrently.

A bipolar transistor switch with inductive load is driven with reverse- base current during turn-off. At the end of the turn-off, a situation may develop depending on the value of the inductive load and reverse-base drive where the collector current as well as the collector base blocking voltage may exceed both critical current and voltage at the same time. This study permits the evaluation of analytical expressions for critical current density, critical voltage, and the minimum second breakdown current of a BJT switch as a function of critical inductance, load inductance, reverse-base drive and device parameters.

List of Figures

List of Tables

xi

CHAPTER 1

INTRODUCTION

1.1 Current mode Second Breakdown

Second Breakdown is the major cause of failures of transistors in operation. It manifests itself internally by a sudden collapse of the collector-emitter voltage and the loss of control of the base drive. Analysis of damages (local melting of both silicon and contacting materials) reveals that the crystal is subjected to considerable heating over a very small area which can only originate from an extreme concentration of the collector current density.

Two different mechanisms have been identified as being the causes of such current concentration. Thermal mode second breakdown (TSB) is induced by a local regenerative thermal runaway which develops as soon as a certain critical temperature has been reached within the active area of the device [1]. Although most types of second breakdown observed are probably caused by heating, an alternative theory to explain second breakdown was proposed by Grutchfield and Moutoux [2]. Hower and Reddi [3] extended the theory by further consideration of the final low voltage test. The second mechanism of failure of the device is electrically initiated and is called the current mode second breakdown (CSB).

The current mode second breakdown is at least theoretically , a non-thermal mechanism. It occurs when the collector current density exceeds a certain critical value while the device is subjected to a high voltage. The explanation involves the role of the free carrier space-charge in the depletion layer of the collector-base junction. At high current densities, this free charge can no longer be disregarded in relation to the charged impurities. When the collector current density exceeds the critical value $J_o = q v_s N_{DC}$, where v_s is the saturated carrier velocity, q is the

electronic charge and N_{DC} is the collector doping density, the maximum electric field intensity does not occur at the metallurgical junction rather it occurs at the interface between the lightly doped collector region and the highly doped substrate. This maximum electric field increases with the collector current density and may reach values leading to avalanche multiplication. Current crowding occurs at the center of the emitter in this condition of operation. The crowding is caused by the center of the base-emitter junction being at a higher forward voltage than the edge, since the emitter to base contact resistance leads to a potential gradient in the base. This condition is shown in Fig. 1.1 . The injected current in turn, gets multiplied in the collector, increases the base current, and reinforces the central crowding. Hence, by regenerative action, the current increases rapidly and, at the same time, is confined to a narrower area. It is believed that the regenerative nature of this mechanism will ultimately allow high current densities to be reached within the centeral region. In a circuit incorporating a collector load resistance this will cause a fall in collector voltage. This condition leads ultimately to the low voltage state associated with current mode second breakdown. The final voltage is below open-base breakdown voltage, BV_{CEO}. Holes generated by impact ionization near the collector-substrate interface not only produce a strong emitter-base forward bias voltage but at the same time neutralize the charge of electrons and thereby decrease the electric field in regions outside the avalanche injection zone. As a result the terminal voltage decreases with increase of current density. Fig. 1.2 shows the experimentally observed I-V characteristics for three mesa transistors of different sizes [4]. The electronic mechanism acts extremely rapidly, since no additional heating is required. Its effect, however, is to accelerate the internal temperature rise and hence transfer to a thermally activated second breakdown condition.

1.2 CSB in power transistors with inductive loads

The reverse-bias (turn-off) characteristics of fast switching $n^+pn^-n^+$ power transistors have become important as these devices are used in increasing numbers

Base   Emitter   Base

I_E

.... electron current

n-p-n device   ——— hole current
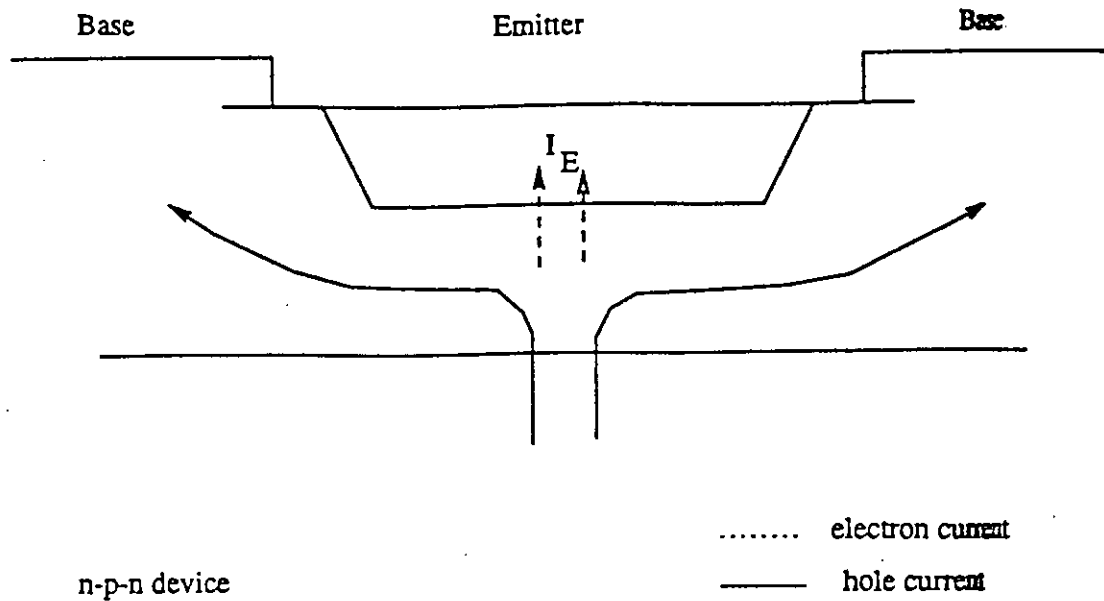
Fig.1.1. Central injection from returning avalanche current.

I_c (amps)

r_m / 9·5 μm   6·5 μm

W_{epi}

r_m

5 μm

$J = 9 \times 10^9 A/m^2$

$J = 9·5 \times 10^9 A/m^2$

3

2

1

0

0   10   20   30   40   50

V_{CE} (volts)
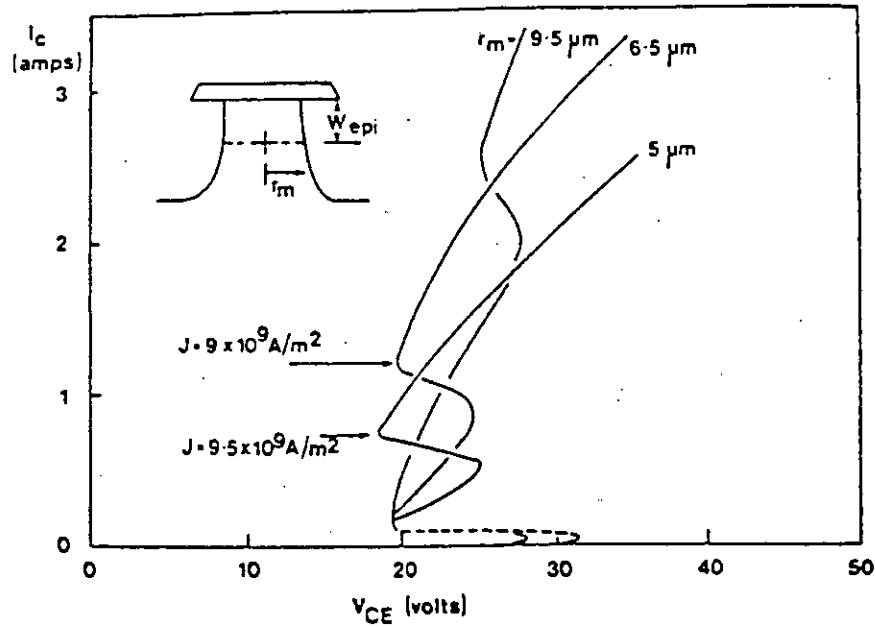
Fig.1.2. I-V characteristics obtained on small area mesa n^+pnn^+ epitaxial transistors pulsed into current mode second breakdown

3

as high speed switches in switching power supplies and motor drives. But power transistor switches operating with inductive loads are often damaged by CSB. Research to improve the device and circuit operating characteristics and to obtain a better model and understand their operation is continuing. The turn-off switching dynamics are very difficult to model and understand [5]. The most severe impediment to this research is to obtain a quantitative analysis of failure due to avalanche injection during turn-off. However, during turn-off, current is localized in the center of the emitter density and terminal voltage can reach levels which trigger avalanche injection. The liability of expitaxial bipolar $n^+pn^-n^+$ power transistor switches to CSB during turn-off in inductive circuits calls for focussing attention not only on new drive concepts besides structural improvements and dependence of external inductive loads on reverse base drive and device parameters.

The transistor switch in the on-state is normally biased into hard saturation by applying a base current larger than $\dfrac{I_C}{h_{feo}}$, where h_{feo}, is the value of the common emitter maximum current gain in the active region of operation. The hard saturation boundary is considered as a favorable location for the operating point in the on-state. Indeed this location still allows important collector current to flow while the apparent resistance of the device is kept to its minimum. The charge distribution within the collector is shown in Fig. 1.3.

When the operating point enters the hard saturation region, the collector current approaches its final on-state value and no longer varies. The charge is stored both in the base and all over the lightly doped collector which constitute a single electrical un-differentiated region.

At the beginning of the turn-off process, this charge begins to decrease — excess holes are removed via base current and excess electrons drift toward the collector

4
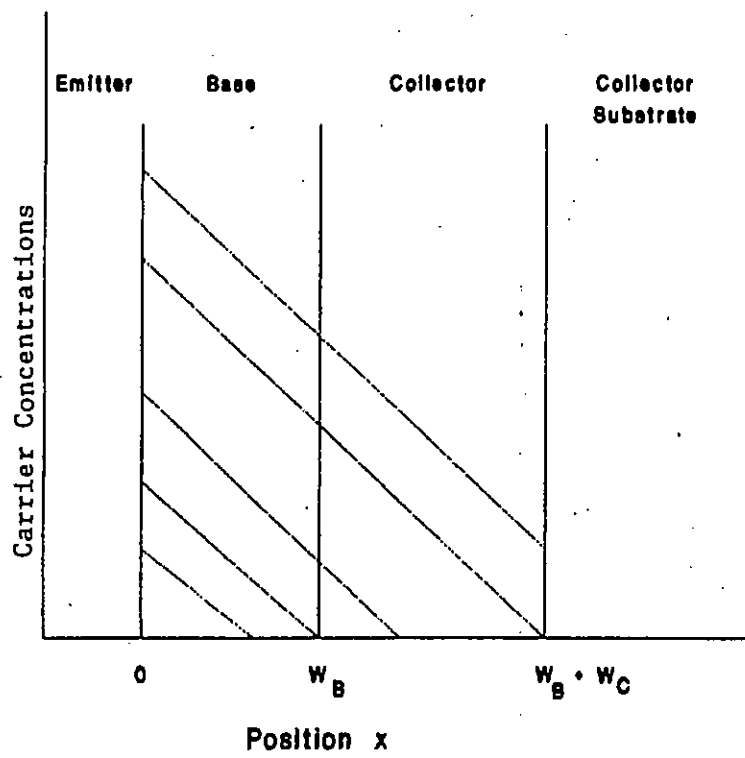
Fig. 1.3 Carrier concentration distributions

and contribute to the collector current. The carrier profile will shift toward the collector-base metallurgical junction untill a point is reached where the collector voltage begins to increase (Fig. 1.4). Further flow of reverse-base drive I_{BR} would deplete pn^- (collector-base) junction and causes a large incrase in voltage. On the other hand, any change in voltage across the inductive load will be caused by a corrsponding change in collector current. With the formation of depletion width the effective base shrinks and the center of the emitter diffusion may be strongly forward biased by the flow of transverse reverse base drive, I_{BR}. A situation may arise where the current density at the center of the emitter diffusion as well as the terminal voltage may reach their critical values required for triggering CSB.

1.3 Summary of the dissertation

The power transistors have now come of age and are already the preferred devices for a large number of medium-power, medium-frequency applications, i.e. choppers, inverters, switching power supplies, pwm motor control circuits etc. In spite of the fact that its current-handling and voltage blocking capabilities are far lower than those of thyristors, it has the advantage of a total controllability at turn-off as well as at turn-on with a relatively fast switching velocity. But one major difficulty with the epitaxial bipolar transistor is its susceptibility to failure by turning off inductive loads. One of the mechanisms which initiates failure is due to the avalanche generation (impact ionization) of carriers within the collector region of the transistor. In this case the disturbance can escalate rapidly (within nano sec.) and it is usually difficult to provide circuit protection that can respond quickly enough to avoid device degradation. A few numerical works have been done to study the role of inductive load on initiating avalanche injection. For the purpose of conceptual understanding of the role of . inductance, circuit analysis and design to prevent the occurrence of CSB, the numerical model is overly cumbersome. In this thesis in studying the failure of the transistor switch with inductive loads, a simplified analytical treatment is carried out.
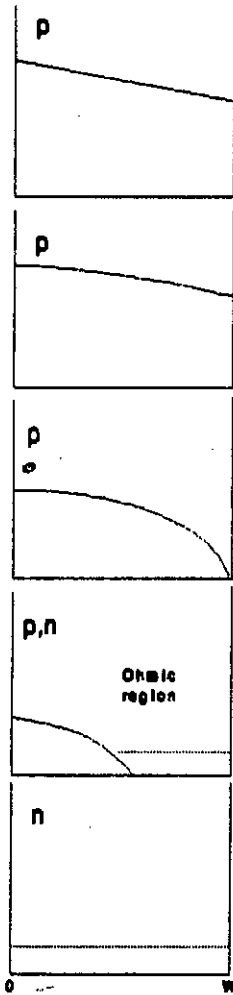
Fig. 1.4 Time sequence of hole-electron
concentrations in n⁻ region

7

The reverse base current flowing through the base produces a lateral voltage drop. The emitter current is localized at the center of the emitter stripe where a high current density will be reached. In chapter 2, a simple analytic expression for collector current under pinched-in condition of the emitter is derived. When the current density at the center of the emitter diffusion equals the critical current density J_{crit}, the collector current will be considered as the minimum value of second breakdown current to initiate avalanche injection. The analysis shows that the current constriction becomes severe for larger values of reverse-base drive, I_{BR}.

Two-dimensional models of turn-off dynamics of power transistors have dealt mainly with the internal behavior of transistors during turn-off and did not include a carrier generation term in the continuity equations for currents. In chapter 3, analytical expressions for critical voltage and critical cutrent density are derived, accounting for the effects of field and current density on the carrier generation. These analytical solutions are simple and require little computation to evaluate critical voltage and critical current. The results are in good agreement with the experimental data.

At the end of turn-off process, the device voltage will rapidly rise and the collector current will decrease. The rate of decrease of the current will be controlled by the external inductive load and the reverse base-drive during the fall of collector current. The collector current and voltage might intersect the I-V characteristic of the device on $I_{SB,min}$ and V_{crit}. In chapter 4, a relationship of external load inductance L, with reverse-base drive I_{BR}, V_{crit} and $I_{SB,min}$ is established. The analysis shows that for a given reverse-base drive of a particular device, there exists a critical inductance L_c. If $L > L_c$, the device goes into CSB.

CHAPTER 2

EMITTER CURRENT CROWDING AT THE ONSET OF
CURRENT MODE SECOND BREAKDOWN

2.1 Introduction

The use of power transistors and other semiconductor devices is often limited
Ωby a phenomenon called "Second Breakdown" which is marked by an abrupt
decrease in device terminal voltage with a simultaneous internal constriction of
current. In a practical transistor, second breakdwon generally starts with current
localization to the center of the emitter stripe caused by lateral voltage drop across
base spreading resistance. This is aggravated by nonuniform conduction prior to
turn-off of the epitaxial bipolar transistor operating under reverse-bias condition. In
this chapter a mathematical treatment of the distribution of emitter current density
under reverse-base drive condition is carried out.

2.2 Analysis

When a transistor switch is operated in reverse biased condition, the lateral
base current produces a voltage drop across the emitter base junction. This has
the effect of strongly forward biasing the center of the emitter diffusion and thereby
causing a high emitter current density through the center of the emitter diffusion. If
the concentration of space charge entering the collector exceeds the fixed thermally
ionized impurity concentration, the mobile charge will determine the electric field
within the lightly doped collector. If the collector-emitter voltage V_{CE} is high,
then a situation can develop where the electric field exceeds its critical value for
impact ionization. Multiplication and localized avalanche breakdown occur. The
generated holes will drift towards the base and produce a lateral voltage drop across
the emitter diffusion. This effect encourages a corresponding local increase in the

9

emitter injection (emitter pinch-in). It is proposed that the regenerative nature of this mechanism will ultimately allow high current densities to be reached within the filament. For the purpose of the analysis however, it is sufficient to calculate the emitter current distribution under reverse-base drive. The analysis has, in principle, a close parallel with the earlier work on pinch-in phenomenon in bipolar transistor [6].

Figure 2.1 shows the cross section of a transistor. Holes from the collector enter the base and travel along the emitter producing a lateral voltage drop along the base body.

The lateral current density in the base is given by the expression (Fig.2.2)

$$J_b(x) = -\sigma_b \frac{dV}{dx} \tag{2.1}$$

where, V is the lateral voltage drop.

$$\frac{dV}{dx} = -\rho_b J_b(x) \tag{2.2}$$

where, ρ_b is the base resistivity. In the analysis, the base is assumed to be uniformly doped.
Upon integration

$$V(x) = V(0) - \int_0^x \rho_b J_b(x)\, dx \tag{2.3}$$
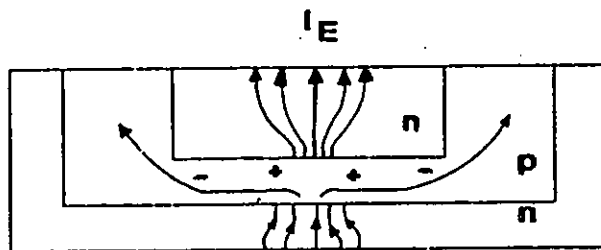
**Fig. 2.1 Pinched-in current distribution
with reversed base current**
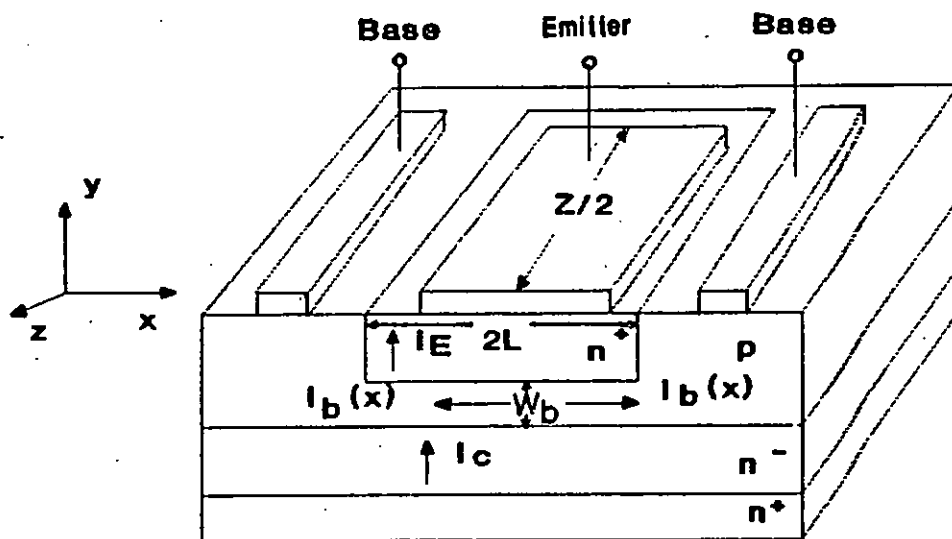
**Fig. 2.2 An $n^+p\ n^-n^+$ epitaxial bipolar transistor
showing current flow.**

11

Defining a parameter

$$G = \frac{dI_b}{dI_e}$$

$$dI_b = G\,dI_e$$

$$= G\,J_e(x)\frac{Z}{2}dx$$

$$\frac{dI_b}{dx} = \frac{GZ}{2}J_e(x)$$

$$\frac{d}{dx}\left[J_b(x)\frac{Z}{2}W_b\right] = \frac{GZ}{2}J_e(x)$$

$$\frac{dJ_b(x)}{dx} = \frac{G}{W_b}J_e(x) \tag{2.4}$$

Differentiating equation (2.4)

$$\frac{d^2 J_b(x)}{dx^2} = \frac{G}{W_b}\frac{dJ_e(x)}{dx} \tag{2.5}$$

The emitter current density $J_e(x)$ is related to $V(x)$ by

$$J_e(x) = J_o\left[\exp\left(\frac{V(x)}{V_t}\right) - 1\right] \tag{2.6}$$

where, J_o is the reverse saturation current density and $V_t = \frac{kT}{q}$.

The first term in the bracket of eqn. (2.6) is much greater than the second term. Hence neglecting the second term we get,

$$J_e(x) = J_o\exp\left(\frac{V(x)}{V_t}\right) \tag{2.7}$$

Using eqns. (2.4), (2.5) and (2.7)

$$\frac{d^2 J_b(x)}{dx^2} = \frac{1}{V_t} \frac{dJ_b}{dx} \frac{dV(x)}{dx} \tag{2.8}$$

Combining eqns. (2.2) and (2.8)

$$\frac{d^2 J_b(x)}{dx^2} = -\frac{\rho_b}{V_t} J_b(x) \frac{dJ_b(x)}{dx}$$

Integrating,

$$\frac{dJ_b(x)}{dx} = -\frac{\rho_b}{2V_t} J_b^2(x) + C_1$$
$$= \frac{\rho_b}{2V_t} \left[\frac{2C_1 V_t}{\rho_b} - J_b^2(x) \right]$$

Let

$$A^2 = \frac{2C_1 V_t}{\rho_b}$$

where, A is a constant.

Rewriting,

$$\frac{dJ_b(x)}{dx} = \frac{\rho_b}{2V_t} \left[A^2 - J_b^2(x) \right] \tag{2.9}$$

ΩIntegrating eqn. (2.9)

$$\ln \frac{A + J_b(x)}{A - J_b(x)} = 2A \left[\frac{\rho_b}{2V_t} x + C_2 \right]$$

for $A > J_b(x)$

$$\frac{A + J_b(x)}{A - J_b(x)} = \exp \left(2A \left[\frac{\rho_b}{2V_t} x + C_2 \right] \right)$$

13

On simplification

$$J_b(x) = A \tanh\left[A\left(\frac{\rho_b}{2V_t}x + C_2\right)\right] \qquad (2.10)$$

At $x = 0$,

$$\frac{dV(x)}{dx} = 0$$

Using this boundary condition, from eqn. (2.2) it can be shown that

$$J_b(0) = 0 \qquad (2.11)$$

From eqns. (2.10) and (2.11),

$$C_2 = 0$$

With $C_2 = 0$, eqn. (2.10) can be written in the following form,

$$J_b(x) = A \tanh\left(\frac{A\,\rho_b}{2V_t}x\right) \qquad (2.12)$$

$$I_b(x) = \frac{Z}{2}W_b\,J_b(x)$$

$$= \frac{AZW_b}{2}\tanh\left(\frac{A\,\rho_b}{2V_t}x\right) \qquad (2.13)$$

At $x = L$,

$$I_b(L) = \frac{I_{BR}}{2}$$

where, I_{BR} is the total reverse base current.

$$\frac{I_{BR}}{2} = \frac{AZW_b}{2}\tanh\left(\frac{A\,\rho_b}{2V_t}L\right)$$

14

For power transistors L is very large. For large L,

$$\tanh\left(\frac{A\,\rho_b L}{2V_t}\right) = 1$$

$$A = \frac{I_{BR}}{ZW_b} \tag{2.14}$$

Substituting A in eqn.(2.13),

$$I_b(x) = \frac{I_{BR}}{2}\,\tanh\left(\frac{I_{BR}\,\rho_b}{2ZW_bV_t}\,x\right) \tag{2.15}$$

Substituting eqn.(2.14) into eqn.(2.12) gives

$$J_b(x) = \frac{I_{BR}}{ZW_b}\,\tanh\left(\frac{I_{BR}\,\rho_b}{2ZW_bV_t}\,x\right) \tag{2.16}$$

From eqn.(2.4)

$$J_e(x) = \frac{W_b}{G}\,\frac{dJ_b(x)}{dx} \tag{2.17}$$

Differentiating eqn. (2.16) w.r.t. x and substituting the value into eqn. (2.17) give,

$$J_e(x) = \frac{I_{BR}^2\,\rho_b}{2Z^2W_bV_tG}\,\cosh^{-2}\left(\frac{I_{BR}\,\rho_b}{2ZW_bV_t}\,x\right)$$

Let

$$J_e(0) = \frac{I_{BR}^2\,\rho_b}{2Z^2W_bV_tG} \tag{2.18}$$

$$J_e(x) = J_e(0)\cosh^{-2}\left(\frac{I_{BR}\,\rho_b}{2ZW_bV_t}\,x\right) \tag{2.19}$$

The total emitter current is given by

$$I_E = 2\int_0^L J_e(x)\frac{Z}{2}\,dx$$

$$= \frac{2Z^2W_bV_tJ_e(0)}{I_{BR}\,\rho_b}\,\tanh\left(\frac{I_{BR}\,\rho_b}{2ZW_bV_t}\,L\right)$$

15

For large L,

$$\tanh\left(\frac{I_{BR}\rho_b L}{2ZW_b V_t}\right) = 1$$

$$\text{and} \quad I_E = \frac{2Z^2 W_b V_t J_e(0)}{\rho_b I_{BR}} \tag{2.20}$$

The collector current is given by

$$I_C = I_{BR} + I_E$$

If $I_E \gg I_{BR}$, then

$$I_C = \frac{2Z^2 W_b V_t J_e(0)}{\rho_b I_{BR}} \tag{2.21}$$

At the onset of CSB, $J_e(0) = J_{crit}$. The minimum second breakdown current for a given reverse-base drive I_{BR} can be given by

$$I_{SB} = \frac{2Z^2 W_b V_t J_{crit}}{\rho_b I_{BR}} \tag{2.22}$$

Substituting the value of $J_b(x)$ from eqn. (2.16) into eqn. (2.3), the final form of voltage is

$$V(x) = V(0) - \int_0^x \frac{I_{BR}\rho_b}{ZW_b} \tanh\left(\frac{\rho_b I_{BR}}{2ZW_b V_t} x\right) dx$$

$$= V(0) - 2V_t \left[\ln\cosh\left(\frac{\rho_b I_{BR}}{2ZW_b V_t} x\right)\right] \tag{2.23}$$

2.3 Results

To study emitter current crowding or pinch-in phenomenon in power transistor switches, the mathematical expressions for lateral voltage drop $V(x)$, base current density $J_b(x)$ and emitter current density $J_e(x)$ derived in section 2.2 can be used. For example, consider a transistor with the following data.

16
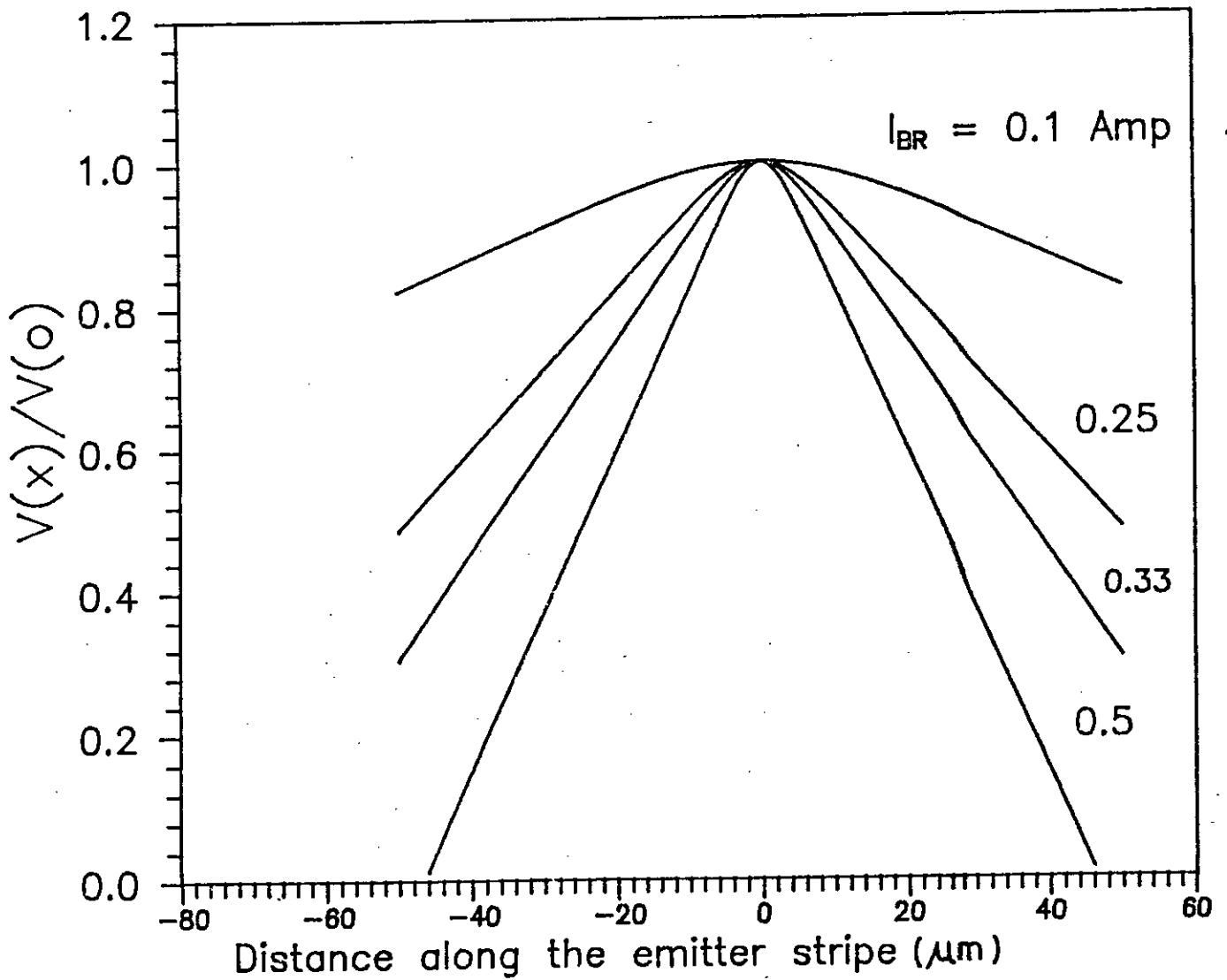
Fig.2.3(a) Normalized lateral voltage drop along the emitter stripe for different values of base current.
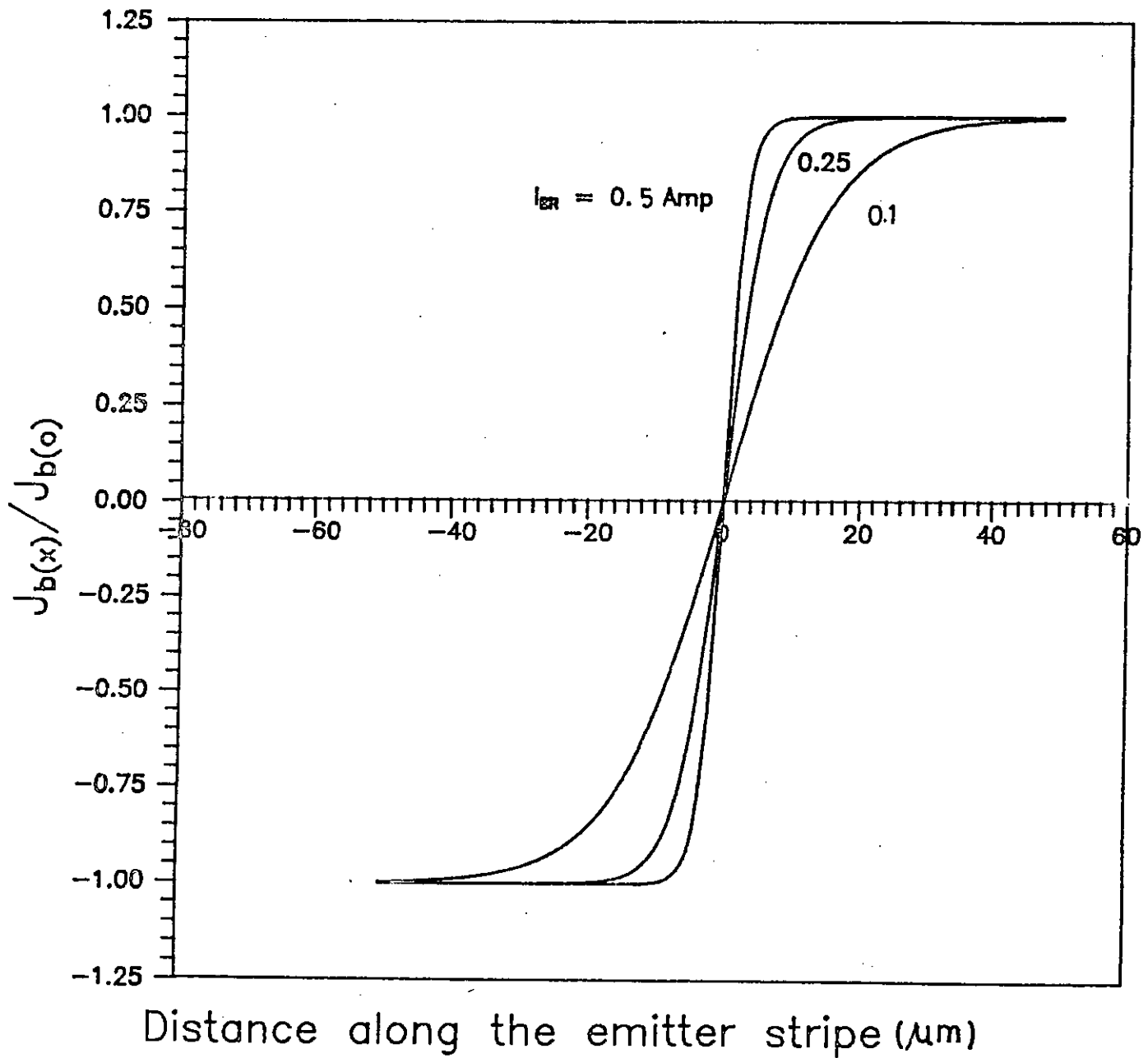
Fig.2.3(b) Normalized base current along the emitter stripe for different
values of base current.
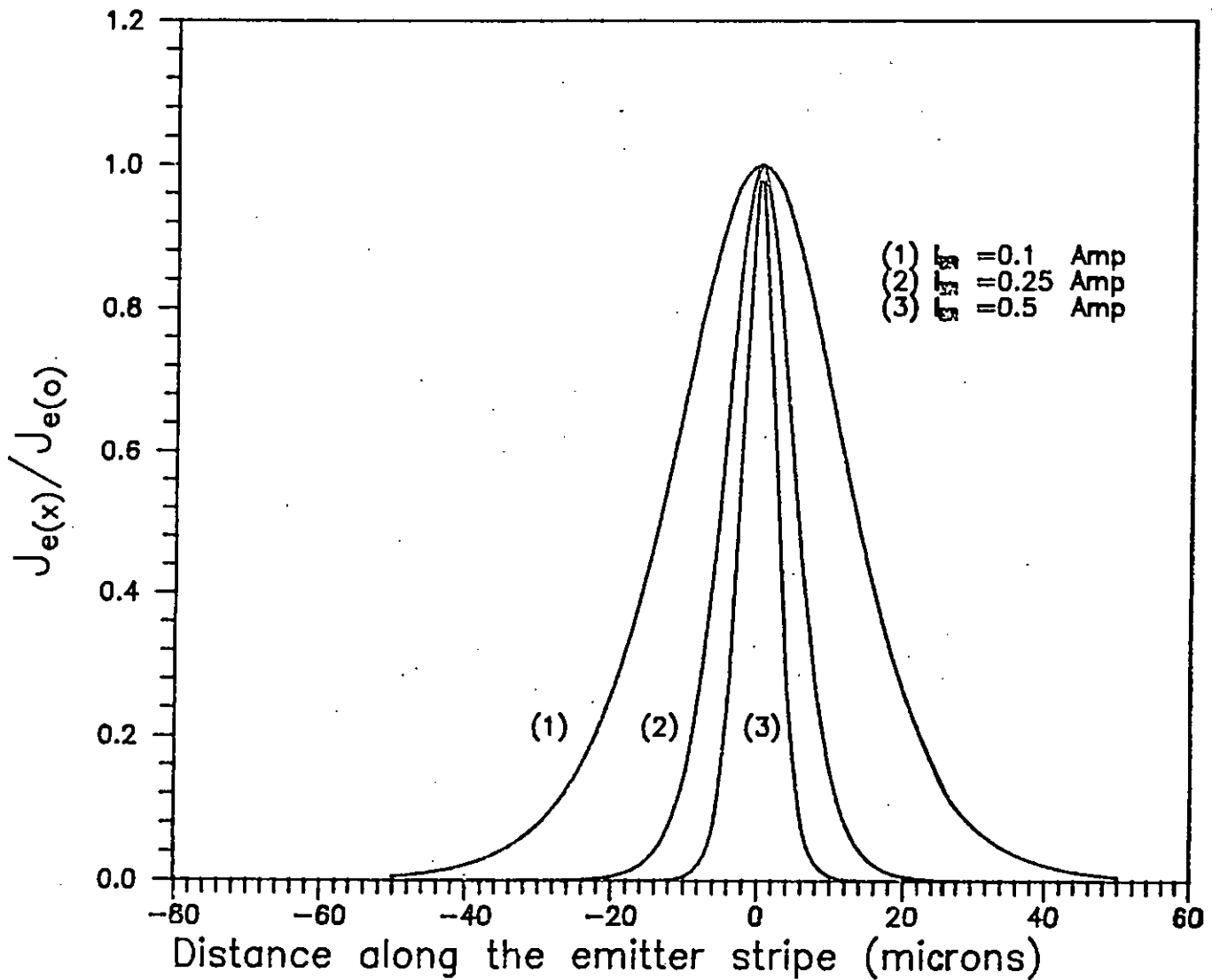
Fig.2.3.(c) Distribution of normalized emitter current density along
the emitter stripe for different values of base current.

5

4

3

$J_{e(x)}(1 \times 10^3 \ A \ cm^{-2})$

2

1

0

$I_{BR} = 0.1 \ A$ 0.25   0.5

-80   -60   -40   -20   0   20   40   60

Distance along the emitter stripe(μm)
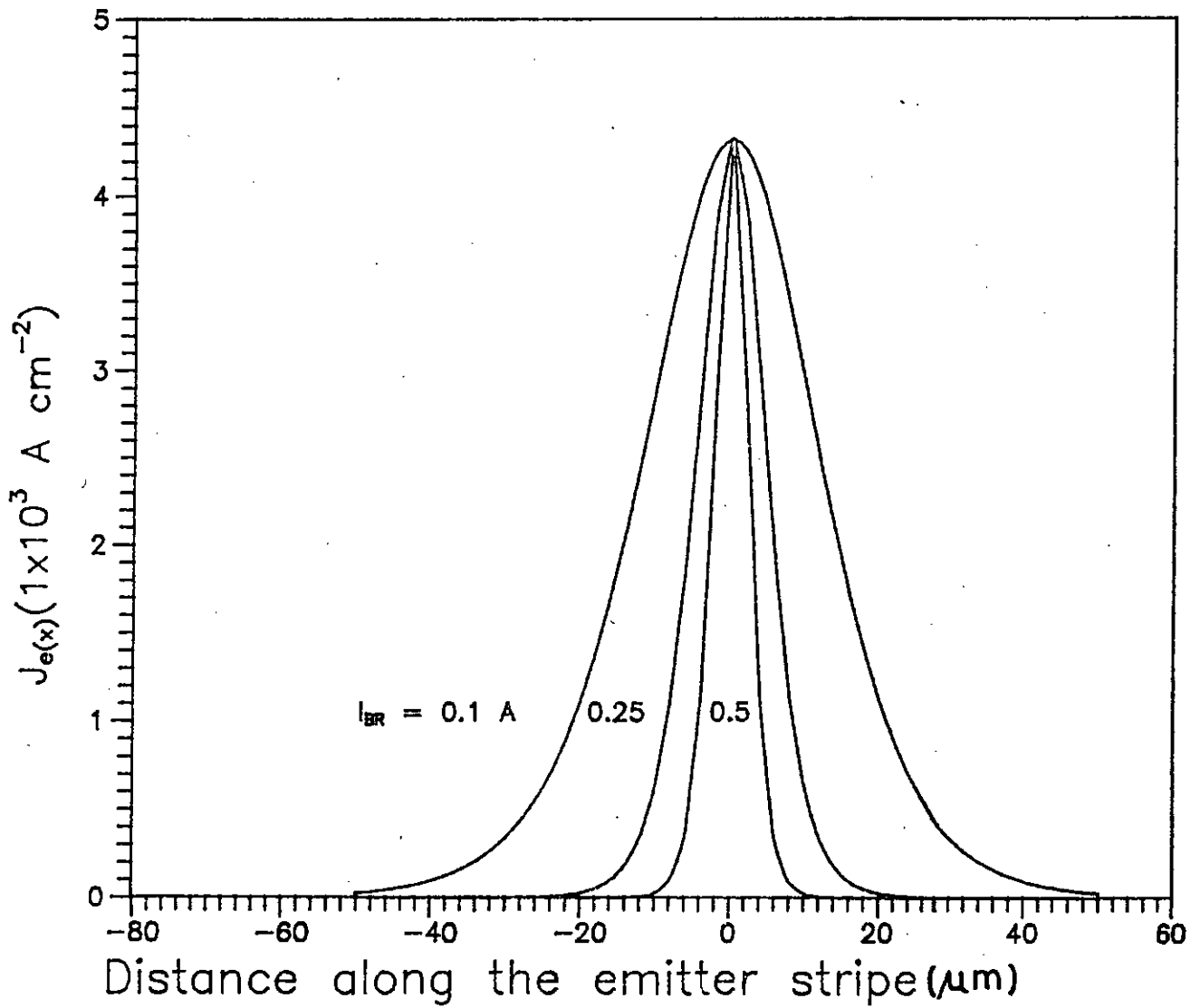
Fig.2.4 Emitter current density along the emitter stripe for different
values of base current.

DATA

Emitter current, $I_E = 30$ Amps

Emitter perimeter, $Z = 4.5$ cm

Base width, $W_b = 5.6 \times 10^{-4}$ cm

Emitter stripe width, $2L = 10^{-2}$ cm

Base resistivity, $\rho_b = 0.85$ ohm-cm

Figure 2.3(a), (b) and (c) show normalized value of lateral voltage $\dfrac{V(x)}{V(0)}$, base current density $\dfrac{J_b(x)}{J_b(0)}$ and emitter current density $\dfrac{J_e(x)}{J_e(0)}$ as a function of emitter stripe length for different values of reverse base currents respectively. While Fig. 2.4 shows $J_e(x)$ as a function of emitter width for different values of I_{BR}.

2.4 Conclusions

In this chapter mathematical expressions needed to explain the pinch-in phenomenon which ultimately leads to current mode second breakdown are derived. The analytical expression for emitter current density in terms of device parameters is important in studying the pinch-in phenomenon. The results in Fig. 2.3(c) indicate that the current constriction becomes severe for large I_{BR}. This is confirmed by the results in Fig. 2.3(a) and (b) which show that for large reverse base current, the center of the emitter stripe is more forward biased than the edge. So at a large reverse base current, the major portion of the emitter current flows through a very narrow region near the center of the emitter diffusion.

CHAPTER 3

ESTIMATE OF CRITICAL VOLTAGE FOR TRIGGERING
CURRENT MODE SECOND BREAKDOWN

3.1 Introduction

Power transistors used in switching applications are very much susceptible to failure due to current mode second breakdown during inductive turn-off. Turn-off is normally accomplished by reversing the base current to sweep out the charge stored in the lightly-doped collector region of an expitaxial $n^+pn^-n^+$ bipolar transistor switch when it is in the " on-state ". Excess electrons drift towards the collector contact where they contribute to the collector current. At the end of storage time, collector voltage begins to increase rapidly but the collector current falls slowly. A situation may arise where the collector voltage and collector current density may reach critical values. Consequently, avalanche injection starts at the n^-n^+ interface. Although a first order solution was given by Krishna and Hower [7], the analysis was only approximate. At low current density levels, the device voltage increases with collector current density. If the current density reaches a critical value, the peak electric field enters the range where avalanche generation becomes significant, and the device shows negative resistance with further increase of current density. The critical point on the J-V characteristic corresponds to the intersection of positive and negative branches of the J-V relationship.

The negative resistance is controlled by current sharing between electrons and holes in the saturated drift velocity region, and also by the type of junction (contact). An n^+n^- contact blocks the egress of holes and the negative resistance of n^+nn^+ devices is attributed to the increase of the low field conductivity modulation (due to accumulation of holes near the cathode), and the decrease of the field

22

slope in the saturated velocity region with increase of generated hole near the anode. On the other hand, since a pn (base-collector) junction allows the holes to escape through the junction, the negative resistance of an $n^+pn^-n^+$ transistor is contributed only by the saturated velocity region. In the later case, a relatively high ionization rate will be required and subsequently demands a high field for producing negative resistance. Krishna and Hower's model did not take into account this role of the junction (contact) in determining the critical current density. However, the disturbance in the existing charge density created by the carrier generation depends on the peak electric field and on the electron current density entering into the multiplication zone. For a particular electron current density, this disturbance increases with the peak electric field. An analysis taking into account this disturbance in charge density will give more accurate results than one that simply assumes a critical electric field. Two-dimensional models of BJT turn-off [8, 9] have dealt mainly with the internal behavior of transistors during turn-off and have not included a carrier generation term in current continuity equations.

In this chapter analytical expressions for critical current density and critical voltage are derived, accounting for the effects of field and current density on the carrier generation factor. These analytical solutions are simple and require little computation to evaluate the voltage and current density, in contrast to a numerical analysis which usually involves large computation times. Also, the analytical solutions are in excellent agreement with experimental results. The epitaxial layer of thickness L, is divided into three regions as shwon in Figure 3.1 . The first region, near the collector-base junction, is characterized by a linear velocity-field dependence up to a saturation value v_s, equal for both carriers. This approximation leads to electron and hole mobilities lower than the actual ones; however, it does not modify substantially the results because over the most of the collector the fields are above E_s, the minimum electric field with which carriers move with saturated velocities. In region 2, both electrons and holes move with their saturated velocities and avalanche generation is negligible. However, this region terminates at the

23

Collector Region

Collector Width
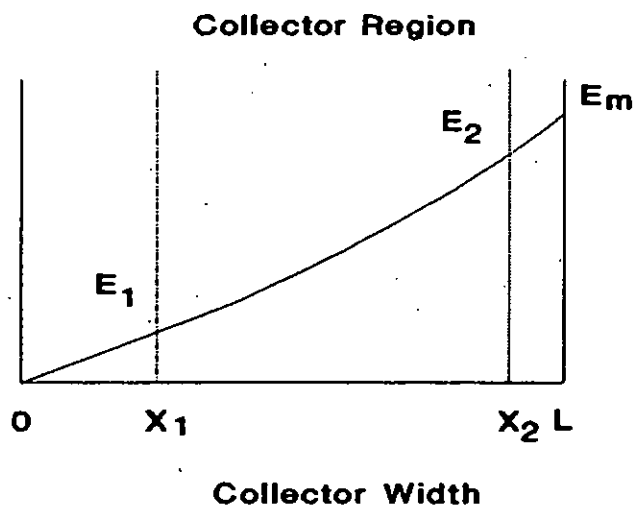
Fig. 3.1 Electric field distribution within the
collector region.

region near the $n^- n^+$ interface where carrier generation cannot be neglected and a disturbance in charge density occurs within a thin zone near the interface at the onset of avalanche injection. In this analysis, E_s is taken to be equal to $2 \times 10^4 \ V cm^{-1}$.

3.2 Analysis

An exact solution of the avalanche injection problem is rather complicated. However, an analytical solution can be easily obtained using the folowing assumptions:

a. Recombination is negligible throughout the collector region.

b. The density of thermally generated carriers is small compared to the collector doping concentration, N_{DC}.

c. Electron and hole saturated drift velocities are equal.

d. Only the drift component of current need to be considered.

The diffusion component is important only at low electric fields, and the numerical analysis [9] shows that the low field region occupies only a small portion of the collector. Since we are dealing with the situation where the electric field everywhere(except in a small region near the base-collector junction)is beyond the onset of saturation, neglecting the effect of diffusion in determining the critical voltage is justified.

The basic equations to be solved are,

$$J = q v_n n + q v_p p \tag{3.1}$$

$$\frac{dJ_n}{dx} = -\frac{dJ_p}{dx} = \alpha J_n + \beta J_p \tag{3.2}$$

$$g = \alpha n + \beta p \tag{3.3}$$

$$\frac{\epsilon}{q} \frac{dE}{dx} = n - N_{DC} - p \tag{3.4}$$

25

where, $n(p)$ electron(hole) density, g is the carrier generation rate, α and β are electron and hole ionization rates respectively.

The boundary value for the electric field is set by the condition existing at $x = 0$, i.e., at the collector-base metallurgical junction at the final state of the turn-off period. During inductive turn-off, the transistor leaves the saturation region by discharging the excess charge from the collector. The final state of turn-off occurs when the junction begins to block. At this point, the current density at the emitter center might exceed the critical current density which triggers avalanche injection. The models of power transistor turn-off dynamics [8,9] show that the electric field is very small at $x = 0$. Therefore, at $x = 0$, electric field is assumed to be zero in the present analysis.

Region 1 $0 \leq x \leq x_1$

In this region the electric field is less than E_s, so the carrier velocities are linear function of the electric field. Holes generated by impact ionization within a very thin layer in region 3 near the $n^- n^+$ interface travel towards the region 1. However, at the onset of avalanche injection hole density can be neglected since for $J > J_o$, $n \gg p$ in this region. In region 1, the velocity is field dependent and therefore, electron density increases with decrease of field to maintain constant electron current density J_{ns} throughout this region.

With the approximations, $n \gg p$ and $n \gg N_{DC}$ at the onset of avalanche injection, eqn. (3.4) and eqn. (3.1) can be written as

$$\frac{\epsilon}{q} \frac{dE}{dx} = n \tag{3.5}$$

$$J = q v_n n \tag{3.6}$$

$$= q \mu_n n E$$

From eqn. (3.6)

$$n = \frac{J}{q \mu_n E} \tag{3.7}$$

26

where, μ_n is the electron mobility.

Substituting n into eqn. (3.5) and rearranging

$$E\,dE = \frac{J}{\mu_n \epsilon}\,dx$$

Integrating,

$$\int_0^E E\,dE = \int_0^x \frac{J}{\mu_n \epsilon}\,dx$$

which gives,

$$E(x) = \left(\frac{2J}{\mu_n \epsilon}\right)^{\frac{1}{2}} x^{\frac{1}{2}} \tag{3.8}$$

Putting the value of $E(x)$ into eqn. (3.7) gives,

$$n(x) = \left(\frac{\epsilon J}{2q^2 \mu_n}\right)^{-\frac{1}{2}} \tag{3.9}$$

At $x = x_1$, $E(x_1) = E_s$ and from eqn. (3.8),

$$E_s = \left(\frac{2J}{\mu_n \epsilon}\right)^{\frac{1}{2}} x_1^{\frac{1}{2}}$$

and

$$x_1 = \frac{v_s{}^2 \epsilon}{2J \mu_n} \tag{3.10}$$

where, $v_s = \mu_n E_s$

The voltage in region 1 can be found by integrating eqn. (3.8) from 0 to x_1. Thus,

27

$$V_1 = \int_0^{x_1} E(x)\,dx$$

$$= \int_0^{x_1} \left(\frac{2J}{\mu_n \epsilon}\right)^{\frac{1}{2}} x^{\frac{1}{2}}\,dx$$

$$= \frac{2}{3} \left(\frac{2J}{\mu_n \epsilon}\right)^{\frac{1}{2}} x_1^{\frac{3}{2}}$$

Substituting the value of x_1 from eqn. (3.10) , V_1 can be written as,

$$V_1 = \frac{v_s^3 \epsilon}{3 J \mu_n^2} \tag{3.11}$$

Region 2 $x_1 \leq x \leq x_2$

The characteristics of region 2 can be summarized as follows :

i. Both electrons and holes move with their saturated velocities.

ii. Electron and hole saturated drift velocities are equal.

iii. Generation of carriers by avalanche multiplication is negligible except in the thin layer close to the $n^- n^+$ interface.

For $J > J_o$, eqns. (3.1) and (3.4) can be written as,

$$J = q v_s (n + p) \tag{3.12}$$

$$\frac{\epsilon}{q} \frac{dE}{dx} = n - p - N_{DC}$$

$$= 2n - \frac{J + J_o}{q v_s} \tag{3.13}$$

Within Region 2, the contribution of the generated carriers can be neglected. With this assumption and integration of eqn. (3.2) leads to the charge density n, as seen by

$$n = n_s + \int_{x_1}^{x} g \, dx$$

From which eqn. (3.13) is rewritten as,

$$\frac{\epsilon}{q} \frac{dE}{dx} = 2n_s - \frac{J + J_o}{q v_s} + 2 \int_{x_1}^{x} g \, dx$$

By linear solution one can obtains,

$$E(x) = E_s + \frac{q}{\epsilon} \left(2n_s - \frac{J + J_o}{q v_s} \right) (x - x_1) \tag{3.14}$$

In region 2, the carrier densities are almost constant, but carrier generation can no longer be neglected as one approaches the boundary with region 3. In fact, the generation of carriers gives rise to an arbitrary disturbance in the existing charge density as one moves into region 3 that causes the change in slope of the electric field. A more accurate result can be obtained if we consider this current density and the disturbance in evaluation of the field rather than simply assigning a critical field and ignoring the effect of this current density on the field profile. In particular, x_2 is defined as the point where the generated carrier density equals the charge considered in this region, that is

$$2n_s - \frac{J + J_o}{q v_s} = 2 \int_{x_1}^{x_2} g \, dx \tag{3.15}$$

At $x = x_2$, $E(x_2) = E_2$ and from eqn. (3.14)

$$\frac{\epsilon}{q} \frac{E_2 - E_s}{x_2 - x_1} = 2n_s - \frac{J + J_o}{q v_s} \tag{3.15a}$$

The method of determination of the value of E_2 is given in appendix A.

29

Using eqn. (3.15a),

$$\int_{x_1}^{x_2} g\,dx = \frac{\epsilon}{2q}\frac{E_2 - E_s}{x_2 - x_1} \tag{3.16}$$

The voltage across region 2 can be found by integrating eqn. (3.14) from x_1 to x_2. Thus

$$\begin{aligned} V_2 &= \int_{x_1}^{x_2} E(x)\,dx \\ &= \frac{1}{2}\,(x_2 - x_1)(E_2 + E_s) \end{aligned} \tag{3.17}$$

Region 3 $\qquad x_2 \le x \le L$

The generation dominates in region 3 and causes the carrier density to vary along this region. At $x = L$,

$$n = \frac{J_n}{qv_s} = \frac{J}{qv_s} \tag{3.18a}$$

since $p = 0$ at n^-n^+ interface.

With the boundary values mentioned above and integrating eqn. (3.2) from x_2 to L it can be shown that

$$\int_{x_2}^{L} g\,dx = \frac{J}{qv_s} - n_s = \frac{J}{qv_s}\left(1 - \frac{1}{M_n}\right) \tag{3.18}$$

This equation cannot be solved analytically unless further approximations are made on the multiplicatin function. But fortunately in this study, this region is not important. However, for small disturbance in the charge, a linear field distribution throughout this region may be retained. Now with $p = 0$ at n^-n^+ interface,

$$J = J_n = q\,v_{s}\,n(L) \qquad (3.19\text{a})$$

With this boundary value and the assumption of a linear field, using eqn. (3.4) the slope for this field within region 3 can be obtained as

$$\frac{dE}{dx} = \frac{J - J_o}{\epsilon v_{s}} \qquad (3.19)$$

3.2.1 Mathematical expression for critical voltage

The total voltage drop across the region 1 and 2 can be calculated by adding eqn. (3.11) and eqn. (3.17). Then

$$\begin{aligned} V &= V_1 + V_2 \\ &= \frac{v_{s}^3 \epsilon}{3 J \mu_n^2} + \frac{1}{2}(x_2 - x_1)(E_2 + E_{s}) \end{aligned} \qquad (3.20)$$

The electric field at the $n^- n^+$ interface is E_m. At the onset of avalanche injection, the generation is very small and it is useful to further approximate the model by shrinking to zero the third region, so that it acts merely as a boundary condition i.e. injection of holes from $n^- n^+$ junction.

As x_2 approaches L, E_2 approaches E_m. Under this condition eqn. (3.18) can be written as

$$\int_{x_1}^{L} g\,dx = \frac{J}{qv_{s}} - n_{s} = \frac{J}{qv_{s}}\left(1 - \frac{1}{M_n}\right) \qquad (3.21)$$

Using eqns. (3.16), (3.21), and (A.6), E_2 can be written as,

$$E_2 = E_{s} + 2(x_2 - x_1)\left(\frac{J}{J - J_o}\right)\left(\frac{a}{b}\right)E_2{}^2 \exp\left(-\frac{b}{E_2}\right)\left[1 - \frac{2E_2}{b} + \frac{6E_2{}^2}{b^2} - \frac{24E_2{}^3}{b^3}\right] \qquad (3.22)$$

31

Now if $M_n = 1, J = qv_s n_s$

$$\frac{\epsilon}{q} \frac{dE}{dx} = n_s - N_{DC}$$

$$= \frac{J}{qv_s} - \frac{J_o}{qv_s}$$

$$= \frac{J - J_o}{qv_s}$$

Integrating,

$$\int_0^E dE = \int_0^x \frac{J - J_o}{\epsilon v_s} dx$$

gives,

$$E(x) = \frac{J - J_o}{\epsilon v_s} x \qquad (3.23a)$$

The voltage across the device is given by

$$V' = \int_0^L E(x) dx$$

$$= \frac{(J - J_o)L^2}{2\epsilon v_s} \qquad (3.23)$$

The above two equations correspond, respectively, to the negative and positive branches of the J-V characteristic. The critical current density can be calculated by solving eqn. (3.22), eqn. (3.20), eqn. (3.23) and eqn. (3.10).

A simple form for J_{crit} can be obtained for the special case when $L \gg x_1$ and $E_m \gg E_s$ as,

32

$$J_{crit} = J_o + \frac{\epsilon v_s}{L} E_m \qquad\qquad (3.24)$$

3.3 Results

The value of critical voltage and critical current density are calculated by simultaneous solution of eqn. (3.22), eqn. (3.20) and eqn. (3.23) for different values of epitaxial layer thickness and doping concentration. In the calculation, the value of various constants assumed are,

$$E_s = 1 \times 10^4 \ V/cm$$

$$\mu_n = 1450 \ cm^2/V - sec$$

$$\epsilon = 1.045 \times 10^{-12} \ farad/cm$$

$$v_s = 1 \times 10^7 \ cm/sec$$

J_{crit} and V_{crit} as a function of expitaxial layer thickness are shown in Fig. 3.2(a) and (b). respectively J_{crit} decreases with increase of L and increases with increase of doping. On the other hand, V_{crit} increases with L but decreases with doping. This dependence of V_{crit} on N_{DC} shown by this analysis cannot be explained by the analytical model of Krishna and Hower [7]. Fig. 3.2(c) shows the dependence of V_{crit} on N_{DC} for different expitaxial layer thickness, while in Fig. 3.2(d) are plots for voltages as a function of J_{crit} of different expitaxial layer thickness. The critical voltage maintains approximately a linear relationship with expitaxial layer thickness. The analytically calculated values of V_{crit} are compared with experimental data [10] and are found to be in very good agreement with measured values (shown in Table 3.1).

Fig.3.2(a) Dependence of critical current density on epitaxial layer thickness for three values of collector doping density.
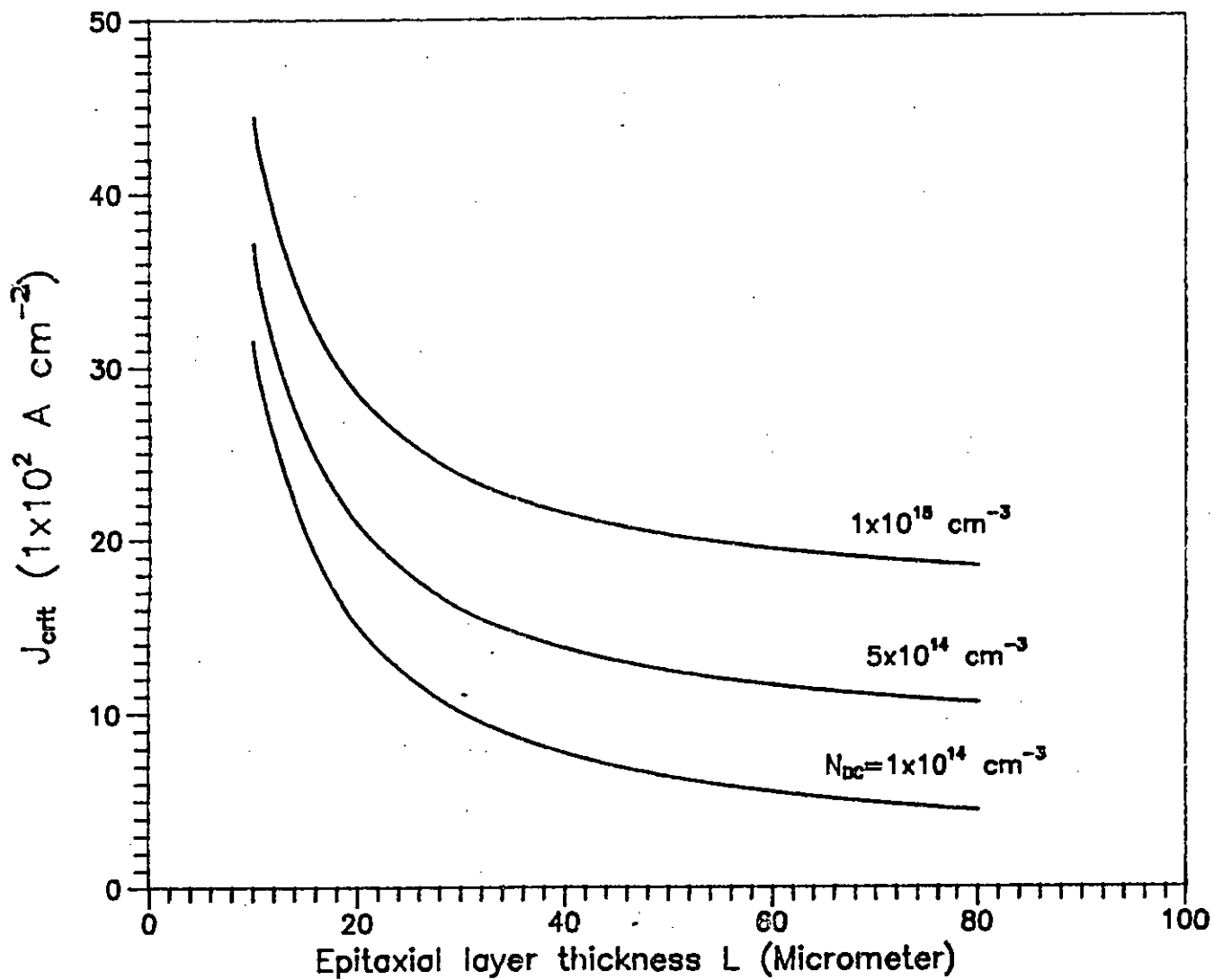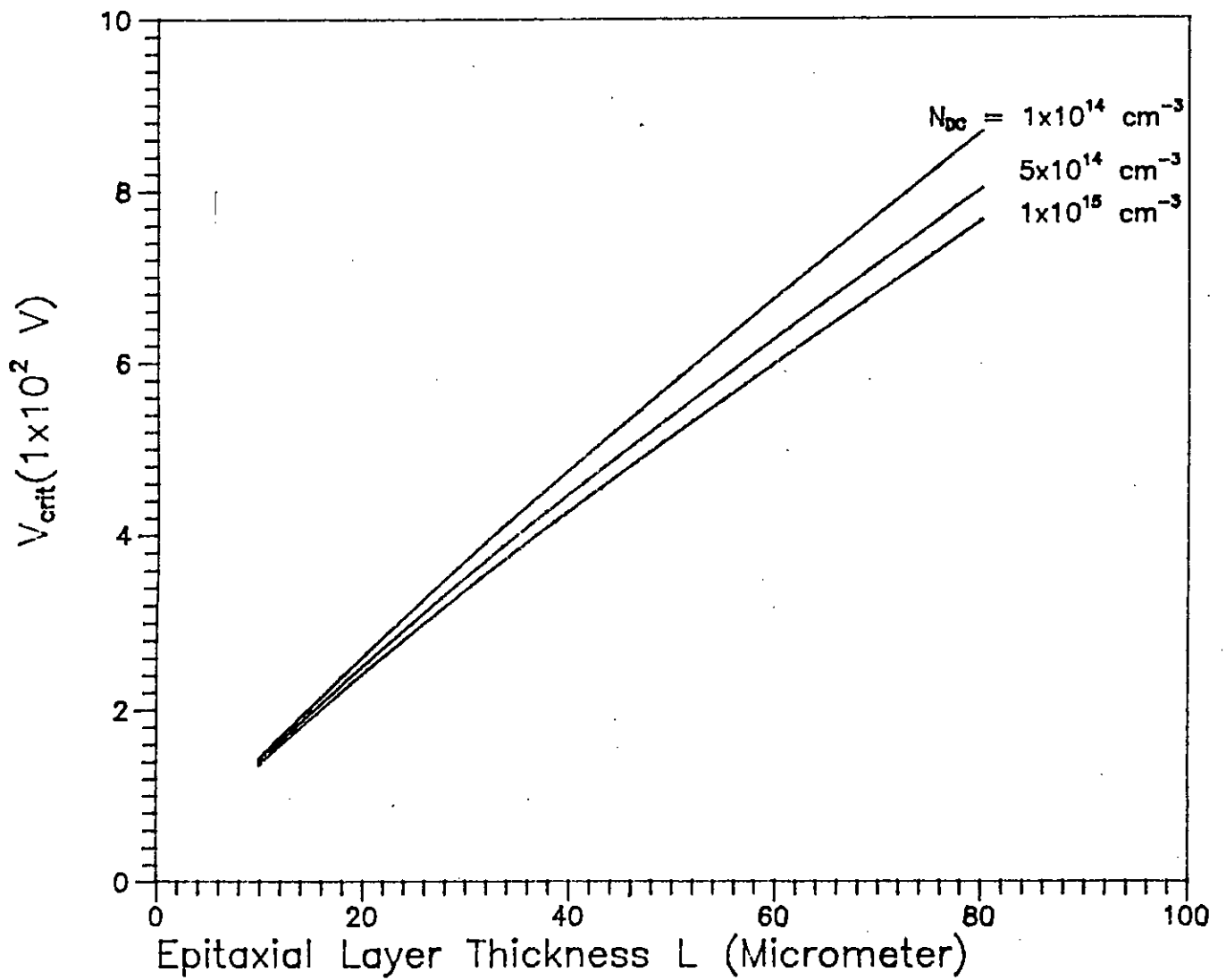
Fig.3.2(b) Dependence of critical voltage on epitaxial layer thickness for three different values of collector doping density.
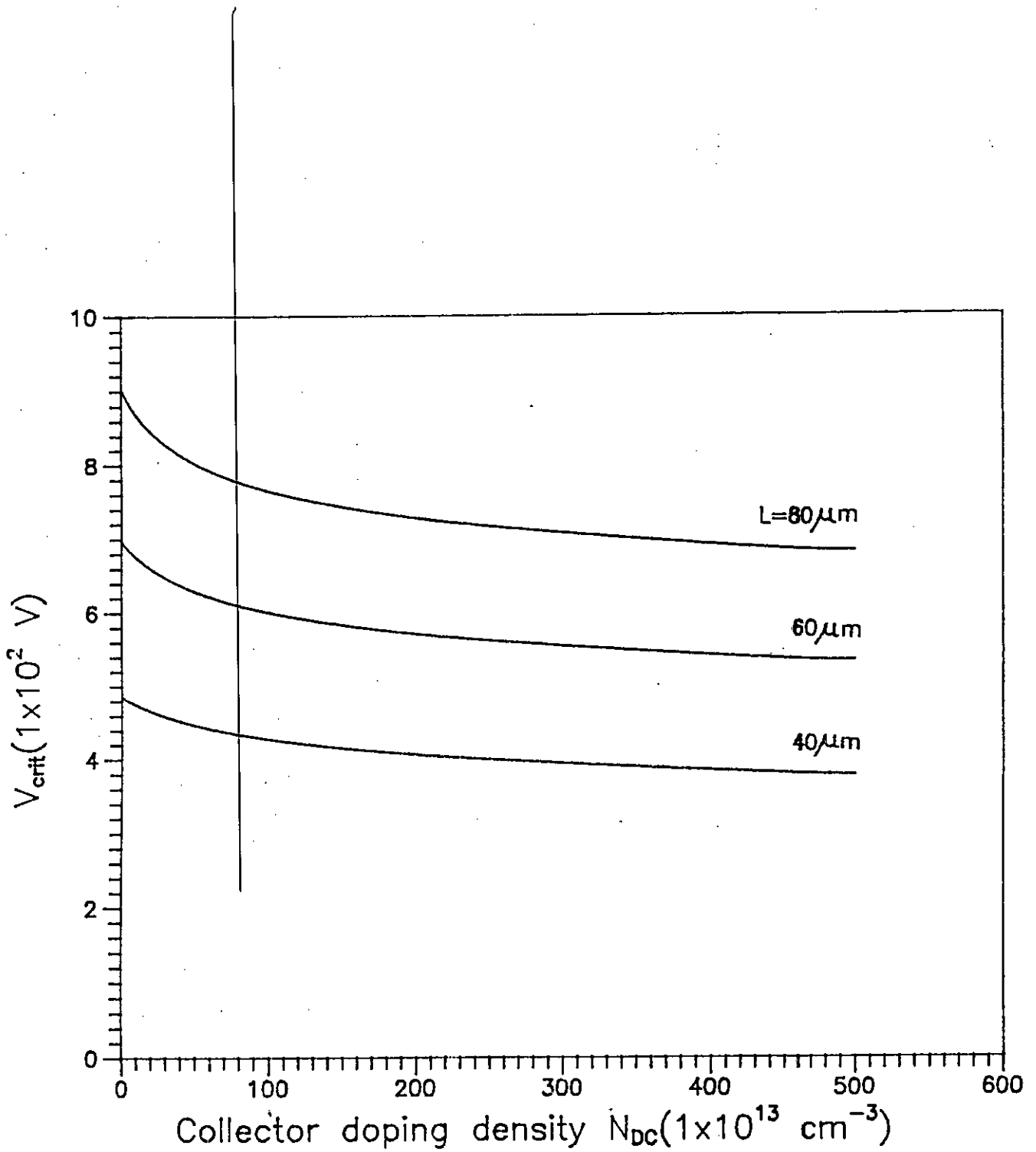
Fig.3.2(c) Dependence of critical voltage on collector doping density
for three different epitaxial layer thicknesses.
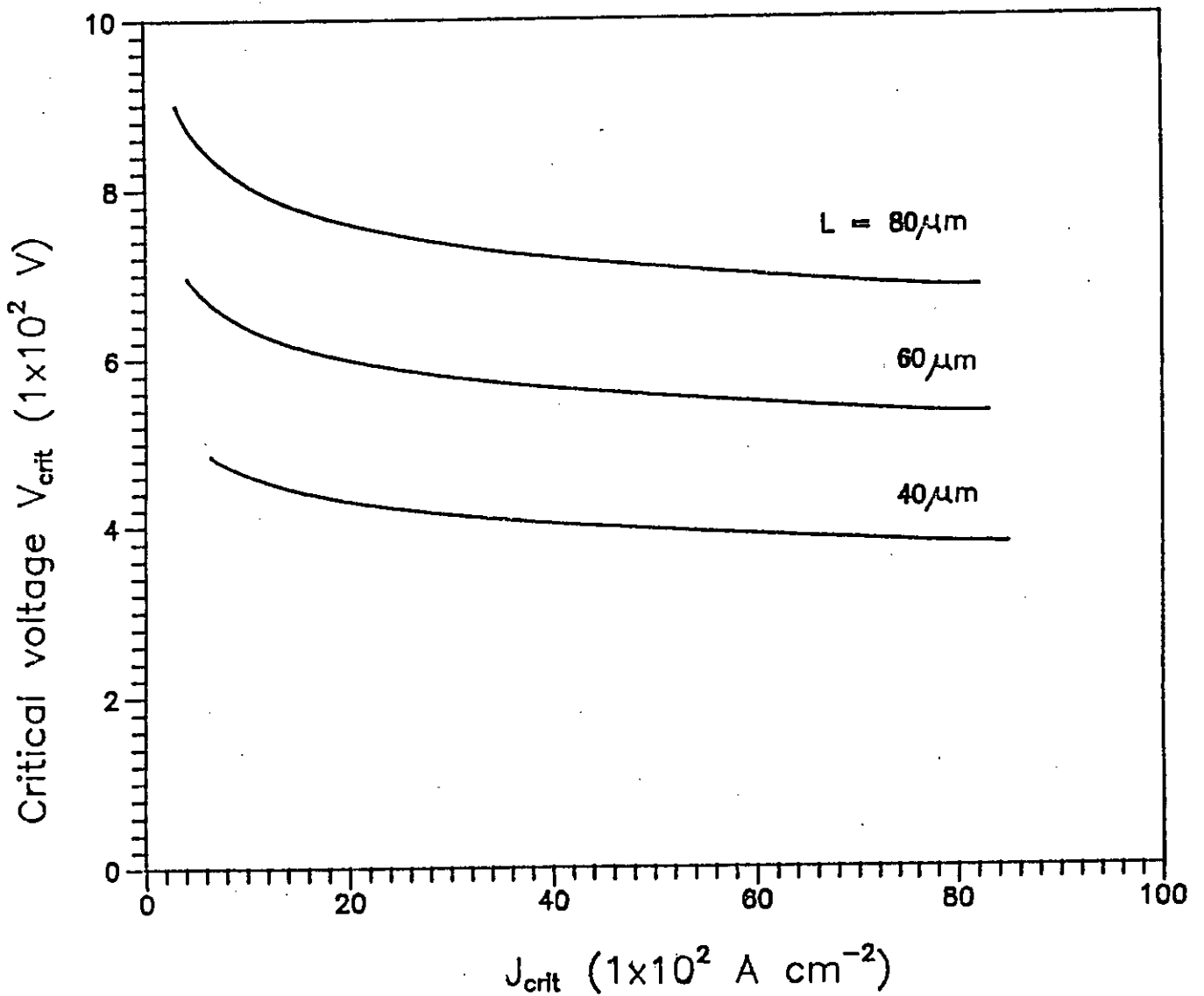
Fig.3.2(d) Dependence of critical current density on critical voltage for three different values of epitaxial layer thickness.

N_{DC} (cm^{-3})	L (μm)	Calculated J_{crit} (A cm^{-2})	Calculated V_{crit} (V)	Measured V_{crit} (V)
2.0×10^{14}	44	861.5	507	620
2.0×10^{14}	46	834.5	527	620
2.0×10^{14}	67	654.8	726	750
2.2×10^{14}	54	778.7	602	680
2.2×10^{14}	80	624.0	842	888
2.3×10^{14}	40	969.2	465	550
2.8×10^{14}	42	1011.8	481	550

Table 3.1 Comparison of calculated critical voltages with measured data [10].

3.4 Conclusions

The critical voltage V_{crit} is unambiguous, and for a given device is determined from circuit conditions only; it expresses unequivocally the second breakdown capability of power transistor switches. This study has computed the magnitude of critical voltage which initiates the current mode second breakdown, where the effects of both the ionization rates and the space-charge produced due to the accumulation of electrons within the collector on carrier generation have been taken into account. The dependence of critical voltage on doping level and epitaxial layer thickness has been investigated. Critical voltage maintains approximately a linear relationship with epitaxial layer thickness.

CHAPTER 4

CRITICAL LOAD INDUCTANCE OF A POWER TRANSISTOR SWITCH

4.1 Introduction

Owing to heat dissipation limitations and power efficiency requirements, the role of bipolar transistors in to-day's applications is mainly confined to that of switches. One of the interesting features of the transistor as a switch is that the power which can be switched is many times the collector dissipation rating of the transistor. This is because in both the open and closed states, the power dissipated in the transistor is low. One major difficulty with the bipolar transistor switch is its suceptibility to failure when turning off the switch with inductive loads. With the increasing use of transistors in inverters and certain other inductive circuits, it becomes imperative to improve device characterization for operation with inductive loads. In this mode of operation, high collector voltage and current are present simultaneously. Second breakdown can occur in situations where base current is flowing in a direction that tends to strongly forward bias the center of the emitter diffusion. In this chapter, analytical expressions are developed to relate the external load inductance to the device parameters.

4.2 Analysis

During on-state, minority carriers are stored in both the base and the lightly doped collector region. When the operating point enters the hard saturation region, the collector current approaches its final on-state value and no longer varies. The switch is driven into off-state by sweeping out all the stored charge from different regions of the base and collector. This is accomplished by reversing the base current. The turn-off problem is particularly important from the standpoint of device operation in power switching applications where the presence of collector inductance can lead to destructive voltage levels during turn-off.

At the initial period of charge removal process, the change of collector current is very small [5]. But in the final state of turn-off when the lightly doped collector region is swept out of minority carriers, the collector inductance will induce a high voltage across the device to prevent the abrupt change in collector current. Since there is no excess minority carriers to sustain this current, the majority carriers will take part in the game. The collector-base junction begins to deplete of carriers and the high voltage appears across this junction. The time dependence of the voltage rise can be obtained from the following one-dimensional analysis.

4.2.1 Voltage rise at the end of the charge storage time

To a good approximation, the space charge within the transition region is contributed only by the uncompensated donor and acceptor ions. The charge density within W is plotted in Fig. 4.1(b). Neglecting carriers within the space charge region, the charge density on the n side is just q times the concentration of donor ions N_{DC}, and the negative charge density on the p side is -q times the concentration of acceptors N_{AB}.

Since the dipole about the junction must have an equal number of charges on either side ($Q_+ = |Q_-|$), the transition region may extend into the p and n regions unequally, depending on the relative doping of the two sides. For a cross-sectional area A, the total uncompensated charge on either side of the junction is

$$qAx_{po}N_{AB} = qAx_{no}N_{DC} \tag{4.1}$$

where x_{po} is the penetration of the space charge region into the p material, and x_{no} is the penetration into n. The total width of the transition region (W) is the
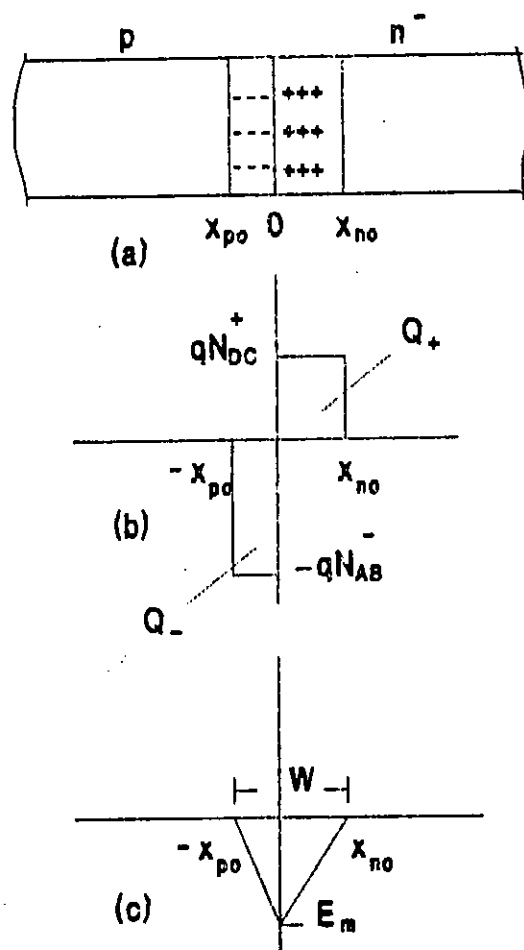
Fig. 4.1 Space charge and electric field distribution within the trasition region.

sum of x_{po} and x_{no}.

The maximum value of the electric field,

$$E_m = -\frac{q}{\epsilon} x_{no} N_{DC} = -\frac{q}{\epsilon} x_{po} N_{AB} \qquad (4.2a)$$

The potential across the junction

$$\begin{aligned}
V &= -\frac{1}{2} E_m W \\
&= -\frac{1}{2} E_m \left(x_{no} + x_{po} \right)
\end{aligned} \qquad (4.2)$$

From eqn. (4.1)

$$x_{po} = \frac{N_{DC}}{N_{AB}} x_{no} \qquad (4.3)$$

Substituting eqn. (4.3) into eqn. (4.2) and simplifying,

$$V = \frac{q}{2\epsilon} N_{DC} \frac{N_{AB} + N_{DC}}{N_{AB}} x_{no}^2$$

If $N_{AB} \gg N_{DC}$, then

$$V = \frac{q N_{DC}}{2\epsilon} x_{no}^2 \qquad (4.4)$$

At the end of the storage time, the excess minority carrier in the induced base region will be swept out. The collector current will start decreasing and the collector-base junction starts blocking the voltage. Holes will be drained out from the base by I_{BR}. The reverse base current I_{BR} is given by

43

$$I_{BR} = qAN_{AB}v_d \qquad (4.5\text{a})$$

where, v_d is the drift velocity of hole.

$$v_d = \frac{I_{BR}}{qAN_{AB}} \qquad (4.5)$$

But the drift velocity can be related to x_{po} by the following equation

$$v_d = \frac{x_{po}}{t} \qquad (4.6)$$

Using eqn. (4.3), eqn. (4.6) can be written as

$$v_d = \frac{N_{DC}}{N_{AB}t} x_{no} \qquad (4.7)$$

Equating eqns. (4.5) and (4.7)

$$x_{no} = \frac{I_{BR}t}{qAN_{DC}} \qquad (4.8)$$

Using eqns. (4.4) and (4.8)

$$V = \frac{I_{BR}^2}{2\epsilon qN_{DC}A^2}t^2$$
$$V = Kt^2 \qquad (4.9)$$

where,

$$K = \frac{I_{BR}^2}{2\epsilon qN_{DC}A^2} \qquad (4.10)$$

44

4.2.2 Second Breakdown current as a function of device parameters and external load inductance

Applying KVL (Fig. 4.2),

$$V_{CE} = V_{CC} - L\frac{di_C}{dt} \qquad (4.11)$$

Neglecting ohmic drop within the collector,

$$V_{CE}(t) = V(t)$$

ΩFrom eqns. (4.11) and (4.9)

$$V_{CC} - L\frac{di_C}{dt} = Kt^2$$

On integration,

$$i_C(t) = \frac{V_{CC}}{L}t - \frac{K}{3L}t^3 + C_1$$

At $t = 0$, $i_C = I_{CM}$.

Using the above boundary condition the expression for collector current can be written as

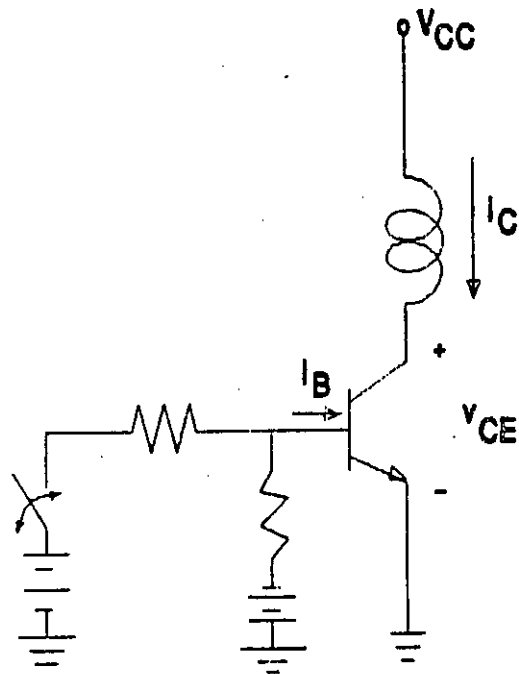$$i_C(t) = I_{CM} + \frac{V_{CC}}{L}t - \frac{K}{3L}t^3 \qquad (4.12)$$

Fig. 4.2 A BJT switch with inductive load

Let at $t = t_1$, the collector-emitter voltage reaches its critical value. Therefore, from eqn. (4.9)

$$V_{crit} = K{t_1}^2$$

$$t_1 = \left(\frac{V_{crit}}{K}\right)^{\frac{1}{2}} \tag{4.13}$$

Using eqn. (4.12) , at $t = t_1$

$$i_C(t_1) = I_{SB} = I_{CM} + \frac{V_{CC}}{L}t_1 - \frac{K}{3L}{t_1}^3 \tag{4.14}$$

Combining eqns. (4.9) and (4.14)

$$I_{SB} = I_{CM} - \frac{K_1}{L} \tag{4.15}$$

where,

$$K_1 = \sqrt{\frac{V_{crit}}{K}} \frac{V_{crit} - 3V_{CC}}{3} \tag{4.16}$$

If the minimum value of the collector current required for occurance of second breakdown is $I_{SB,min}$, then there is a load whose inductance L_c is such that it will cause second breakdown to occur just at the minimum value. So,

$$I_{SB,min} = I_{CM} - \frac{K_1}{L_c}$$

$$L_c = \frac{K_1}{I_{CM} - I_{SB,min}}$$

$$= \frac{V_{crit} - 3V_{CC}}{3(I_{CM} - I_{SB,min})} \left(\frac{2\epsilon q N_{DC} A^2 V_{crit}}{I_{BR}^2}\right)^{\frac{1}{2}} \tag{4.17}$$

47

4.3 Results

Fig. 4.3 shows the relationship between the minimum value of the second breakdown current and the reverse-base current. The value of the second breakdown current decreases with the increase of reverse-base current. The dependence of critical inductance L_c as a function of reverse-base drive I_{BR}, for a given device is plotted in Fig. 4.4. The plot shows that the critical inductance depends upon base drive I_{BR}. The critical inductance decreases with the increase of base drive.

4.4 Conclusions

Constant collector current, corresponding to an inductive load, are usually assumed during the charge removal process. When the minority carriers have cleared, collector current decreases and the collector-base voltage rises. An analysis is presented to show a relationship of second breakdown current with external base drive and inductive loads. The results are presented in a form that allows the selection of base drive to prevent the occurrence of CSB. The expression for critical inductance shows that for a device, its value depends upon base drive and collector peak current. If $L > L_c$, second breakdown cannot be avoided. However, by properly selecting I_{BR}, susceptibility to CSB can be reduced.
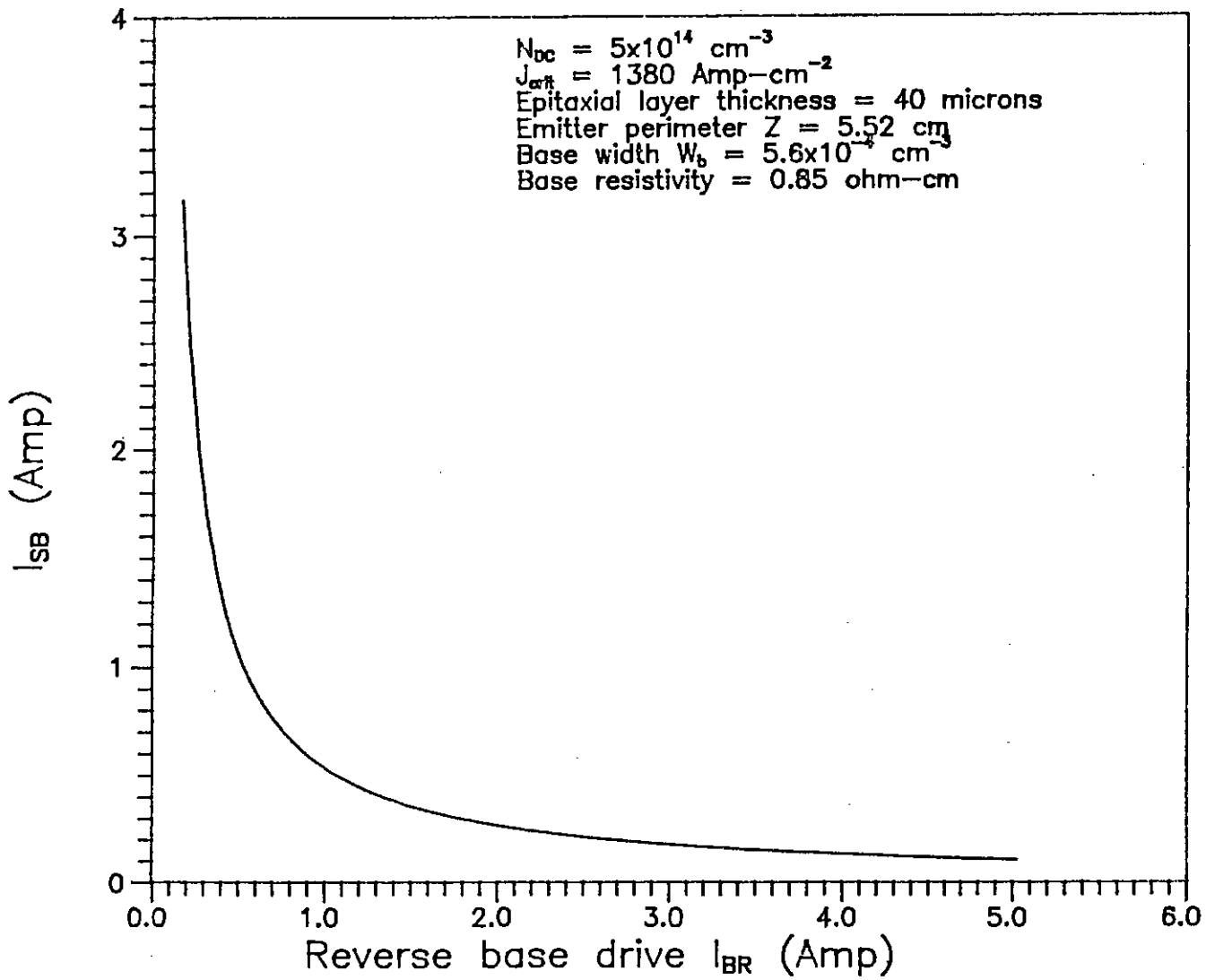
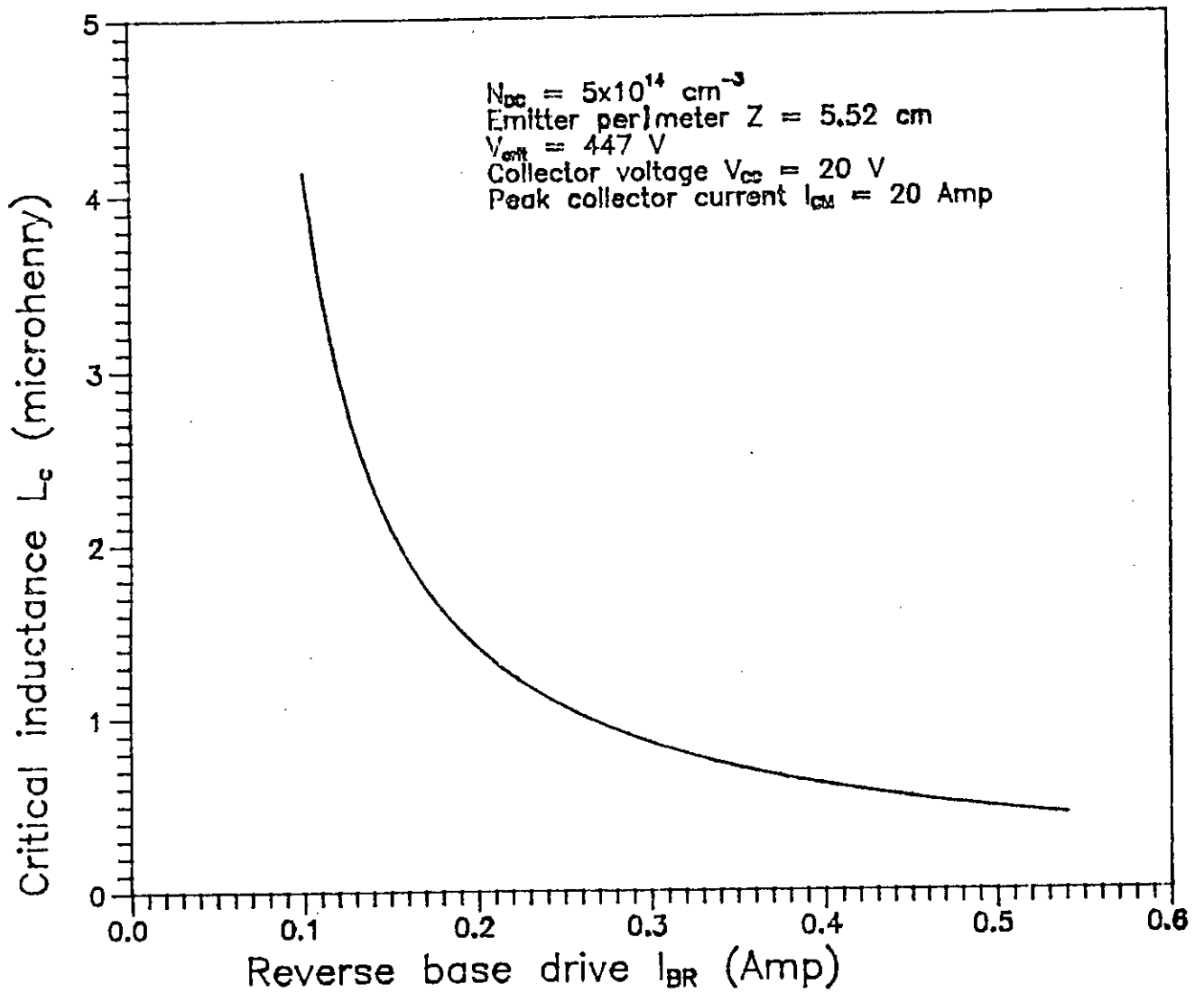Fig.4.3 Second breakdown current I_{SB} as a function of reverse base drive I_{BR}

Fig.4.4 Critical Inductance L_c as a function of reverse base drive I_{BR}

CHAPTER 5

CONCLUSIONS

Transistors often fail during switching even though analytical calculations and predictions, such as power dissipation, based on parameters given by the manufacturer's data sheet should guarantee safe operation. This discrepency arises because the majority of information contained in the data sheet is based on static measurements. Absolute ratings of current, voltage, power and temperature may be specified, but the device may not be able to withstand these conditions if they occur simultaneously.

One of the most critical limitations of a transistor is the magnitude of voltage to which it can be subjected. The voltage at which transistor breaks down is a function of both the individual transistor characteristics. Voltage breakdown characteristics are usually important in circuits which have inductive loads because the high peak powers that are generated influence the mode of transistor operation and the system reliability. Second breakdown is a major limiting factor in the power performance and power handling capability of a transistor. The critical current for the onset of current mode second breakdown increases with collector doping density. This conflicts with the requirement to support a high open-base breakdown voltage, BV_{CEO}. However, by using a double graded collector device, this ambiguity may be solved. An analysis of a transistor with graded collector profiles may be carried out in future.

The designer can do several things to make the device dissipate power under reverse-biased avalanche condition. Reducing the sheet resistance of the base under the emitter helps to conduct more generated currents from collector-substrate interface $(n^- n^+)$ before turn-on occurs. Changes in the lateral geometry of the

51

transistor can minimize the path length of the high sheet resistance base under the emitter, also improving the amount of current that can be conducted before pinch-in occurs.

The turn-off path of a transistor depends on the inductance L and the device parameters. The initial jump in voltage occurs because the inductor current can not change instantaneously. If the voltage rise causes the turn-off path to hit negative-resistance region, the energy delivered by the inductor is greater than the maximum change that can be dissipated by the transistor, the device will be damaged. In this work, the expression for critical inductance is derived which shows that for a device, its value depends upon base drive and collector peak current. If $L > L_c$, second breakdown can not be avoided. However, by properly selecting I_{BR}, the susceptibility to CSB can be reduced.

APPENDIX

CALCULATION OF ELECTRON MULTIPLICATION FACTOR M_n

For multiplication started by elctrons, the electron multiplication factor can be written as [7]

$$1 - \frac{1}{M_n} = \int_0^{\varepsilon_m} \alpha \exp\left(-\int_0^{\varepsilon} (\alpha - \beta)\, dx'\right)\, dx \qquad (A.1)$$

where, α and β are, respectively, electron and hole ionization rates and $\bar{x}_m$ is the width of the avalanche region.

One difficulty in evaluating the integral is the substantial difference in the ionization rates for holes and electrons. An approach which has been fairly successful to assume that individual ionization co-efficients for holes and electrons may be replaced by a single effective ionization co-efficient.

To evaluate the above integration, the effective ionization co-efficient calculated by R. Hall [12] has been used.

$$\alpha' = a \exp\left(-\frac{b}{E}\right) \qquad (A.2)$$

where, $a = 1.54 \times 10^6\ cm^{-1}$ and $b = 1.94 \times 10^6\ V - cm^{-1}$

Therefore,

$$1 - \frac{1}{M_n} = \int_0^{\varepsilon_m} \alpha'\, dx \qquad (A.3)$$

On the assumption of a linear field over the whole multiplication region, the integral can be written bye a variable change

$$1 - \frac{1}{M_n} = \frac{1}{S} \int_0^{E_m} a \exp\left(-\frac{b}{E}\right) dE \qquad (A.4)$$

where, S   is the slope of the field of this region.

Integrating by parts and neglecting the fifth term, eqn. (A.4) can be written as

$$1 - \frac{1}{M_n} = \frac{a}{Sb} E_m{}^2 \exp\left(-\frac{b}{E_m}\right) \left[1 - \frac{2E_m}{b} + \frac{6E_m{}^2}{b^2} - \frac{24E_m{}^3}{b^3}\right] \qquad (A.5)$$

At the onset of avalanche injection, the generation is small and occurs in a very thin region (region 3) close to the $n^- n^+$ interface, where the field slope is $\frac{J - J_o}{\epsilon v_s}$. For small generation, the field profile can be approximated by a straight line since the disturbance created by generated carriers is not significant. With this approximation, we can safely use eqn. (A.5) in our problem. If we taken $S = \frac{J - J_o}{\epsilon v_s}$, then eqn.(A.5) can be written as

$$1 - \frac{1}{M_n} = \left(\frac{a}{b}\right) \left(\frac{\epsilon v_s}{J - J_o}\right) E_m{}^2 \exp\left(-\frac{b}{E_m}\right) \left[1 - \frac{2E_m}{b} + \frac{6E_m^2}{b^2} - \frac{24E_m^3}{b^3}\right] \quad (A.6)$$

Bibliography

1. Ph. Leturcq and C. Cavalier, "A thermal model for high power devices design," IEDM Technical Digest, Washington, pp. 422-428, 1974.

2. H. B. Grutchfield and T. J. Moutoux, "Current mode second breakdown," IEEE Trans. Electron. Devices, ED-13, No. 11, pp. 743-748, 1966.

3. P. L. Hower and B. G. K. Reddi, "Avalanche injection and second breakdown in transistors," IEEE Trans. Electron. Devices, ED-17, No. 4, pp. 320-335, 1973.

4. D. M. Dow and K. I. Nuttel, "A study of the current distribution established in npn epitaxial transistors during current mode second breakdown," Int. J. Electronics, Vol. 50, No. 2, pp. 93-108, 1981.

5. Chenming Hu, "A model of power transistor turn-off dynamics," IEEE Trans. Electron. Devices. ED-27, No. 1, pp. 01-95, 1980.

6. Undergraduate project, "Emitter current pinch-in during current mode second breakdown," Dept. of EEE, Bangladesh University of Engineering and Technology, 1990.

7. S. Krishna and P. L. Hower, "Second breakdown of transistors during inductive turn-off," IEEE Proc. Vol. 61, pp. 393-395, 1973.

8. O. Manck and L. Engl. "Two-dimensional computer simulation for switching a bipolar transistor out of saturation," IEEE Trans. Electron. Devices, ED-22, pp. 339-347, 1975.

9. K. Wang, D. H. Navon, T. Tang and P. L. Hower, "Second breakdown prediction by two-dimensional numerical analysis of BJT turn-off," IEEE Trans. Electron. Devices, ED-33, No. 7, pp. 1067-1072, 1986.

55

10. B. A. Beatty, S. Krishna and M. S. Adley, "Second Breakdown in Power transistors due to avalanche injection," IEEE Trnas. Electron. Devices, ED-23, No. 8, pp. 851-857, 1976.

11. R. Van Overstraeten and H. De Man, "Measurement of the ionization rates in diffused silicon p-n junctions," Solid-State Electron., Vol. 13, No. 5, pp. 583-608, 1970.

12. R. Hall, "The effective carrier ionization co-efficient in silicon p-n junctions at breakdown," Int. J. Electronics, Vol 22, No. 6, pp. 521-528, 1967.